IOPscience iopscience.iop.org

Home Search Collections Journals About Contact us My IOPscience

Wurtzite InP/InAs/InP core–shell nanowires emitting at telecommunication wavelengths on Si substrate

This article has been downloaded from IOPscience. Please scroll down to see the full text article.

2011 Nanotechnology 22 405702

(http://iopscience.iop.org/0957-4484/22/40/405702)

View the table of contents for this issue, or go to the journal homepage for more

Download details:
IP Address: 193.48.219.28
The article was downloaded on 13/09/2011 at 07:35

Please note that terms and conditions apply.

Nanotechnology **22** (2011) 405702 (6pp) doi:10.1088/0957-4484/22/40/405702

Wurtzite InP/InAs/InP core–shell nanowires emitting at telecommunication wavelengths on Si substrate

M H Hadj Alouane[1,2], R Anufriev[1], N Chauvin[1], H Khmissi[2], K Naji[3], B Ilahi[2], H Maaref[2], G Patriarche[4], M Gendry[3] and C Bru-Chevallier[1]

[1] Institut des Nanotechnologies de Lyon (INL)-UMR5270-CNRS, Université de Lyon, INSA-Lyon, 7 avenue Jean Capelle, 69621 Villeurbanne, France
[2] Laboratoire de Micro-Optoélectronique et Nanostructures (LMON), Faculté des Sciences, Avenue de l'environnement, 5019 Monastir, Tunisia
[3] Institut des Nanotechnologies de Lyon (INL)-UMR5270-CNRS, Ecole Centrale de Lyon, Université de Lyon, 36 avenue Guy de Collongue, 69134 Ecully, France
[4] Laboratoire de Photonique et de Nanostructures (LPN), UPR20-CNRS, route de Nozay, 91460 Marcoussis, France

E-mail: nicolas.chauvin@insa-lyon.fr

Received 22 April 2011, in final form 27 July 2011
Published 12 September 2011
Online at stacks.iop.org/Nano/22/405702

Abstract
Optical properties of wurtzite InP/InAs/InP core–shell nanowires grown on silicon substrates by solid source molecular beam epitaxy are studied by means of photoluminescence and microphotoluminescence. The growth conditions were optimized to obtain purely wurtzite radial quantum wells emitting in the telecom bands with a radiative lifetime in the 5–7 ns range at 14 K. Optical studies on single nanowires reveal that the polarization is mainly parallel to the growth direction. A 20-fold reduction of the photoluminescence intensity is observed between 14 and 300 K confirming the very good quality of the nanowires.

(Some figures in this article are in colour only in the electronic version)

1. Introduction

In the past few years, III–V semiconductor nanowires (NWs) have attracted considerable interest due to their intriguing physical properties and potential in nanoelectronics and optoelectronics [1, 2]. Moreover, the NW growth using the vapour–liquid–solid (VLS) method [3] is well adapted to grow III–V semiconductors on silicon (Si) substrate, giving to the NW technology a great potential for monolithic integration of optoelectronics and photonics on Si [4–6]. Metal–organic chemical vapour deposition (MOCVD) [7, 8] and molecular beam epitaxy (MBE) [9, 10] have already been reported for the growth of III–V NWs using VLS mechanism. By changing the material during the growth process, the VLS method allows the fabrication of heterostructures in both axial and radial directions and allows one to intentionally dope the NWs [11, 12]. Several works have been based on studies of InAs/InP core–multishell [13, 14] and heterostructure [15, 16] NWs grown on InP substrates. However, detailed investigation of the optical properties of such structures on Si substrates has not been yet reported except for catalyst free MOCVD growth of core–shell InGaAs/GaAs quantum well nanoneedles on Si [17]. Such a study is very important for future monolithic integration of III–V optoelectronic devices as lasers or diodes with Si based electronic components.

In this context, we report on the optical properties of core–shell InP/InAs/InP NWs grown on (001)- and (111)-oriented Si substrates by VLS assisted solid source MBE (SSMBE). In particular, 1.3 and 1.55 μm emission wavelengths can be reached by varying the InAs growth time, which is particularly interesting for the fabrication of emitters in the telecommunication band.

2. Experimental details

The InP/InAs/InP NW samples were grown on Si(001) and Si(111) substrates by VLS SSMBE using Au–In particles

 © 2011 IOP Publishing Ltd Printed in the UK & the USA

obtained by the dewetting of a Au film at 700 °C. The NWs were grown at 400 °C with a V/III beam equivalent pressure (BEP) ratio of 16. The growth begins with 10 mn of InP growth. A growth interruption of 10 s is realized by closing the indium shutter. During this interruption, the phosphorus flux is switched to arsenic flux. Then, the growth of the InAs insertion is done by opening the indium shutter for a growth time of 10, 20, 30 and 40 s for samples A, B, C and D, respectively. After a 10 s growth interruption for the arsenic/phosphorus flux switching, the structure is completed with 10 mn of InP growth. Similar structures were grown on Si(111) substrates for growth times of 20, 30 and 40 s for samples B′, C′ and D′, respectively. High angle annular dark field scanning transmission electron microscopy (HAADF-STEM) imaging was carried out on the NWs from the different samples. The optical properties of the InP/InAs/InP NWs were characterized by PL spectroscopy. The PL measurements were carried out in two different set-ups using a conventional lock-in technique. The samples were mounted in a closed-cycle temperature-controlled He cryostat and were excited with continuous wave off resonant excitation. The PL signal was dispersed through a monochromator and collected using a thermoelectrically cooled InGaAs photodetector or a liquid nitrogen cooled InGaAs detector with cut-off wavelengths of 1.7 and 2.2 μm, respectively. To investigate the lifetime of the QW, time-resolved PL (TRPL) measurements were performed at 14 K using a pulsed laser emitting at 515 nm with a 50 MHz repetition rate. The photoluminescence of the NWs is analysed by a spectrometer and a synchronized streak camera with a temporal resolution of 20 ps. The optical properties of single NWs are studied with a micro-PL set-up. The excitation was provided by a continuous wave He–Ne laser at 632.8 nm and by a microscope objective focusing the excitation power with a spot size of $\approx$4 μm. The sample was mounted in a He-flow cryostat at about 10 K. The PL emission was collected by the same microscope objective and sent to a monochromator equipped with a nitrogen cooled InGaAs photodiode array detector.

3. Structural properties

With the growth conditions that we have used, SEM images show that the NWs have a mean diameter of about 60–80 nm and a length in the 2–3 μm range. Figure 1 shows a HAADF-STEM image of a typical 75 nm diameter NW from sample A. As evidenced by the selected area electron diffraction (SAED) patterns (not shown), the NWs have a wurtzite (Wz) structure with the [0001] axis along the growth direction for both InP and InAs materials, as often observed for VLS grown III–V NWs [16, 18, 19]. HAADF-STEM measurements reveal that the NWs have a hexagonal section with $\{11\bar{2}0\}$ facets (so called a-plane). It is known that a- and m-planes are stable facets due to their low surface energy. The fact that a-planes are favoured in these core–shell NWs could be a consequence of the strain generated by the radial growth of Wz InAs QW into the Wz InP NWs. Due to the high V/III BEP ratio that we have used, no stacking faults or cubic segments were observed in the NWs. We observe the formation of a thin InAs quantum

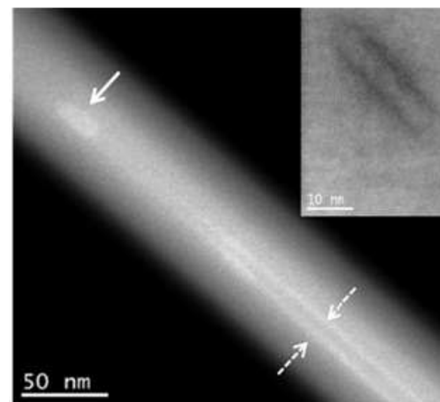

Figure 1. HAADF-STEM image of a NW from sample A; insets: close-up view of the InAs segment.

well (QW) (marked with dashed arrows) a few monolayers (MLs) thick. This QW is surrounded by an inner 7 nm thick InP core and an outer 30 nm thick InP shell formed during the subsequent InP growth. A similar observation has already been reported by Mohan *et al* [13] on InP/InAs/InP core–multishell NWs grown by selective area MOVPE on patterned InP(111)A substrates. We can also observe an inserted InAs segment (marked with a solid arrow) about 20 nm in length. This is due to the axial growth of InAs at the 400 °C growth temperature. In the InAs segment, the central region has a uniform As content but it gradually drops towards the InP interface. Actually, the strain between InP and InAs induces a deformation of the atomic planes near the interfaces, which introduces an additional contrast in the images allowing us to locate the interfaces [16].

4. Photoluminescence investigation of InP/InAs/InP NWs

Low temperature PL spectra of the NW samples grown on Si(001) are shown in figure 2(a). No major modifications are observed in low temperature PL spectra of the NWs grown on Si(111) substrates (figure 2(b)). On Si(001), the maximum peak energy is shown to decrease from 0.98 to 0.78 eV when the InAs growth time increases from 10 to 40 s. The PL redshift in InAs/InP QWs or quantum dots have already been observed and commonly attributed to the increase of the InAs thickness or height, respectively [20, 21]. The spectra of samples consist of multiple peaks in the 0.8–1.3 eV range. This behaviour can be due to the integer ML thickness fluctuation of the radial InAs QW, as observed in two-dimensional InAs/InP QWs [20, 21].

In the case of samples A, B and C, the emission of the InAs segments is assumed to be negligible as compared to the emission of the radial QWs, due to the huge difference between the length of the inserted InAs segments (lower than 100 nm) and the surface of the radial QWs (length more than 600 nm). The situation could be different in the case of sample D where the length of the InAs segments measured by STEM is in the range of 140–150 nm. Further investigations are required in order to conclude on this issue.

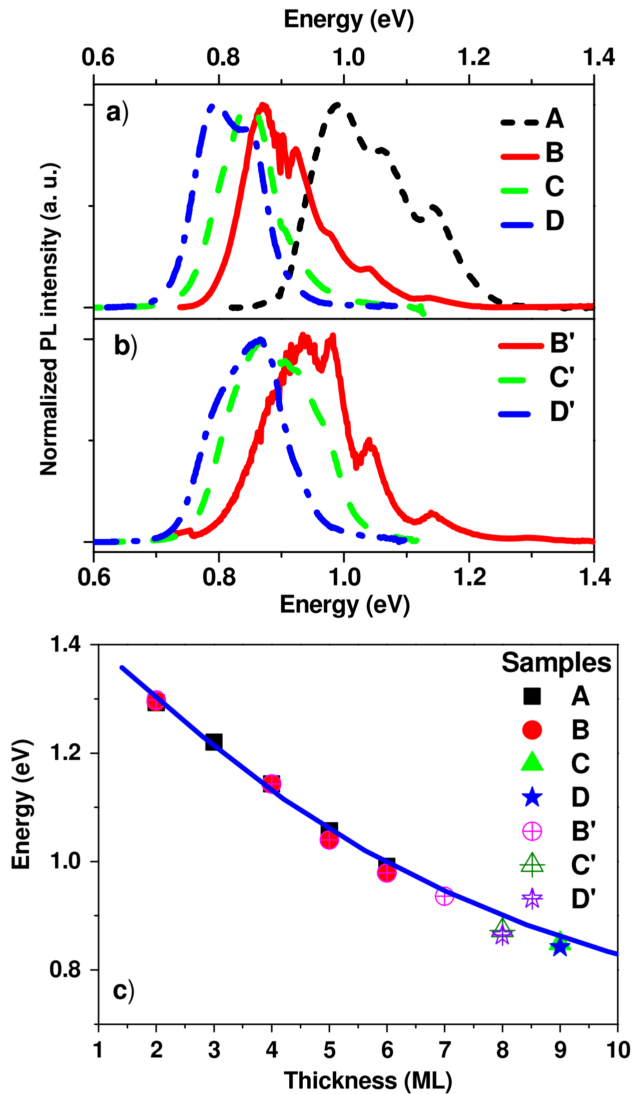

Figure 2. 14 K PL spectra of InP/InAs/InP NW samples grown on (a) Si(001) and (b) Si(111) substrates, for various InAs growth times. (c) Energy of the peaks as a function of the InAs/InP QW thickness. The blue line is the theoretical calculation assuming a ZB InAs/InP QW.

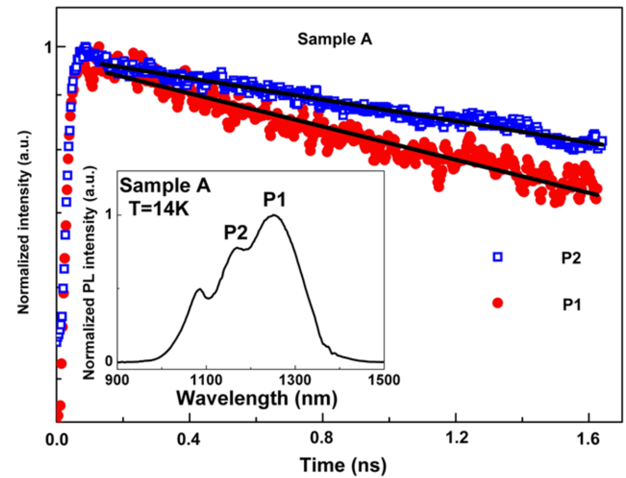

Figure 3. Lifetime decay curves for peaks P_1 (filled circles) and P_2 (empty squares) of sample A measured at 14 K. The black lines show the corresponding fit. Inset: 14 K PL spectra of sample A.

To confirm the assumption of PL emission due to integer ML thickness fluctuation of the QWs, the ground state of an InAs/InP QW is calculated as a function of its thickness using a two-band $k \cdot p$ model where the effect of the strain in the wells is taken into account by coupling the conduction band and light-hole band. The calculation is difficult to perform in the case of Wz InAs/InP QW due to the lack of information about key parameters such as the valence-band and conduction-band deformation potentials, or the spontaneous polarization in Wz InAs and Wz InP materials. Thus, the calculations are performed using the zinc-blende (ZB) parameters of InAs and InP, as approximation already done by other groups working on Wz NWs [13]. In the present study, the QWs are grown on the a-plane of InP; thus non-polar InAs QWs are obtained which reinforce the approximation. The blue line in figure 2(c) shows the theoretical value of the ZB InAs/InP QW ground state as a function of the number of MLs. To be able to compare the ZB QW with the Wz QW, the calculation is performed using a ML thickness equal to $a_{\mathrm{WZ}}^{\mathrm{InAs}}/2 = 0.214$ nm which is the thickness of one ML of Wz InAs material grown on an a-plane. The experimental results are reported in figure 2(c) assuming that the highest energy peak (sample B′) has a thickness of 2 ML. The experimental results are correctly fitted by the theoretical calculation despite the fact that the Wz InAs band gap is expected to be greater than the ZB one. The Wz InAs band gap is not well known: theoretical and experimental values in the 0.47–0.54 eV range have been reported for the Wz band gap [22–24]. The good matching between the experimental and theoretical results could be explained by the fact that the electron effective mass is greater in the Wz InAs phase than in the ZB one. An experimental result has shown a twofold increase of the electron effective mass for the Wz InAs as compared with the ZB one [5]. This is in agreement with a theoretical study which also predicts an increase of the Wz InAs electron effective mass [24]. Such an increase generates a redshift of the QW emission which seems, in our study, to approximately compensate the blueshift due the bigger band gap.

To investigate the lifetime of the QWs, time-resolved PL (TRPL) measurements are performed at 14 K (figure 3). The NWs are excited with a 3 mW average power at 50 MHz. Due to limitations in the detection range of the TRPL set-up (0.3–1.4 μm), we focus on the lifetime of sample A with NWs emitting around 1.3 μm at 14 K.

Figure 3 shows the dynamics for peaks P_1 and P_2 shown in the inset of figure 3. Due to the slow recombination rate of the QWs as compared with the 50 MHz repetition rate, the following equation is used to fit the intensity decay:

$$I(t) = I_1(\exp(-t/\tau_0) + \exp(-(t + \Delta t)/\tau_0))$$

where I_1 is a constant, τ_0 is the lifetime and Δt is the 20 ns delay between two excitation pulses. The second exponential in the equation is used to take into account the carriers generated by the previous laser pulse and still present in the QW. Lifetimes of 5 ns and 7 ns are measured for peaks P_1 and

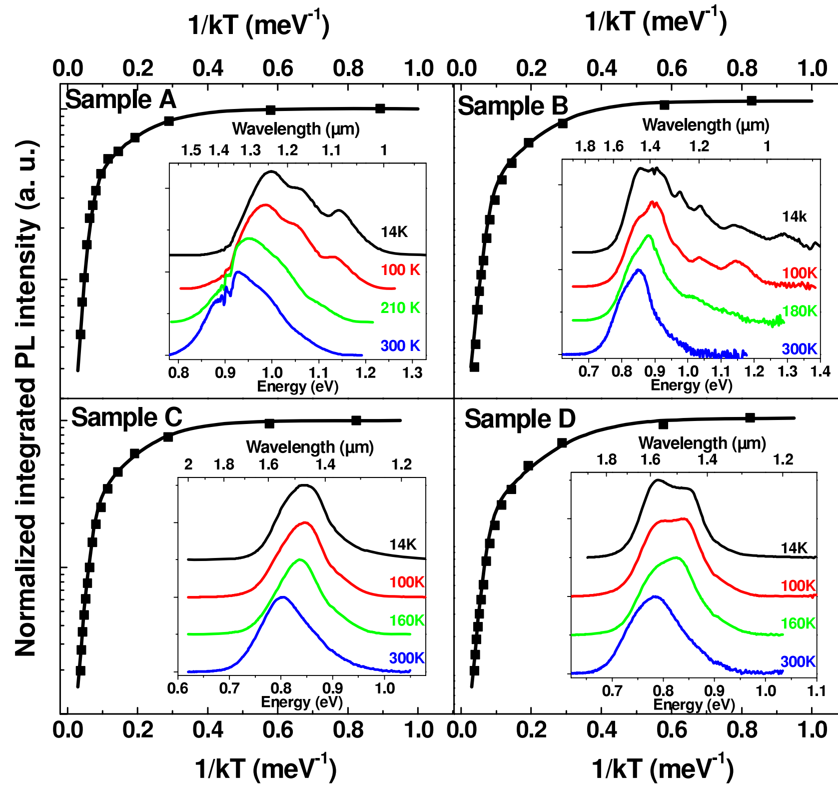

Figure 4. The Arrhenius plot of the integrated PL intensity of the whole emission band for samples grown on Si(001) substrates. Symbols show experimental data and the solid line shows the corresponding fit. Inset: (solid line) temperature induced changes in the PL spectra of these samples.

P_2, respectively. These lifetimes are at least three times longer than the 1.5–1.7 ns lifetimes measured in ZB InAs/InP(001) quantum wells at low temperature [14, 25]. A 16 ns lifetime has already been reported for InP/InAs/InP core–multishell NWs emitting at 1.2 eV and has been associated with a type II recombination [26]. In our case, the PL experiments have revealed a type I alignment. Two assumptions can be made to explain the origin of the long lifetime. The first assumption is a decrease of the spontaneous recombination rate due to the geometry and size of the NWs. Theoretical papers have shown that the spontaneous emission of an in-plane dipole located on the axis of an infinitely long NW is strongly reduced if $D \ll \lambda$, where D is the diameter of the NW and λ the emission wavelength of the dipole [27, 28]. For our samples, the condition $D \ll \lambda$ is fulfilled, but the dipole is not in the centre of the NW. The second hypothesis relies on the fact that the radial InAs QW is grown on the a-plane of Wz InP which means that the QW is parallel to the c-direction. Along this direction a polarization charge distribution is expected and a small electric field can be created depending on the length of the QW [29].

More insight into the heterostructure NW optical properties can be ensured through the investigation of the temperature dependence of the integrated PL intensity. Figure 4 shows the evolution of the integrated PL intensity recorded in NWs grown on Si(001) substrates as a function of temperature between 14 and 300 K. A 20-fold reduction of the PL intensity is measured between 14 and 300 K for sample A. A fit of the experimental data can be performed using the multi-channel Arrhenius equation [30]:

Table 1. Best fit parameters for the calculated curves of figure 4.

Samples	A_1	E_1 (meV)	A_2	E_2 (meV)
A	3.3	**10**	300	**76**
B	9	**10**	1550	**74**
C	5.5	**10.5**	570	**75**
D	8.5	**9**	1000	**72**

$$I = \frac{I_0}{1 + \sum_i c_i \exp(-\frac{E_i}{k_b T})} \quad (1)$$

where i represents the number of channels involved for carrier thermal escape, k_b is the Boltzmann constant, E_i is the thermal activation energy, I_0 is the PL intensity at 0 K and c_i is a constant. We find that the temperature dependence of the integrated PL intensity can be perfectly fitted by considering two escape channels ($i = 2$). The best fits were obtained using the parameters gathered in table 1. The activation energy shows no systematic variation with InAs growth time. The smaller activation energy E_1 can be attributed to the dissociation of the excitons trapped in the QWs followed by the nonradiative recombination of the carrier defects located in the QWs, as reported previously in the InAs(P)/InP QWs [31, 32]. However, the high temperature activation energy (E_2) is likely to be associated with the carrier thermionic emission

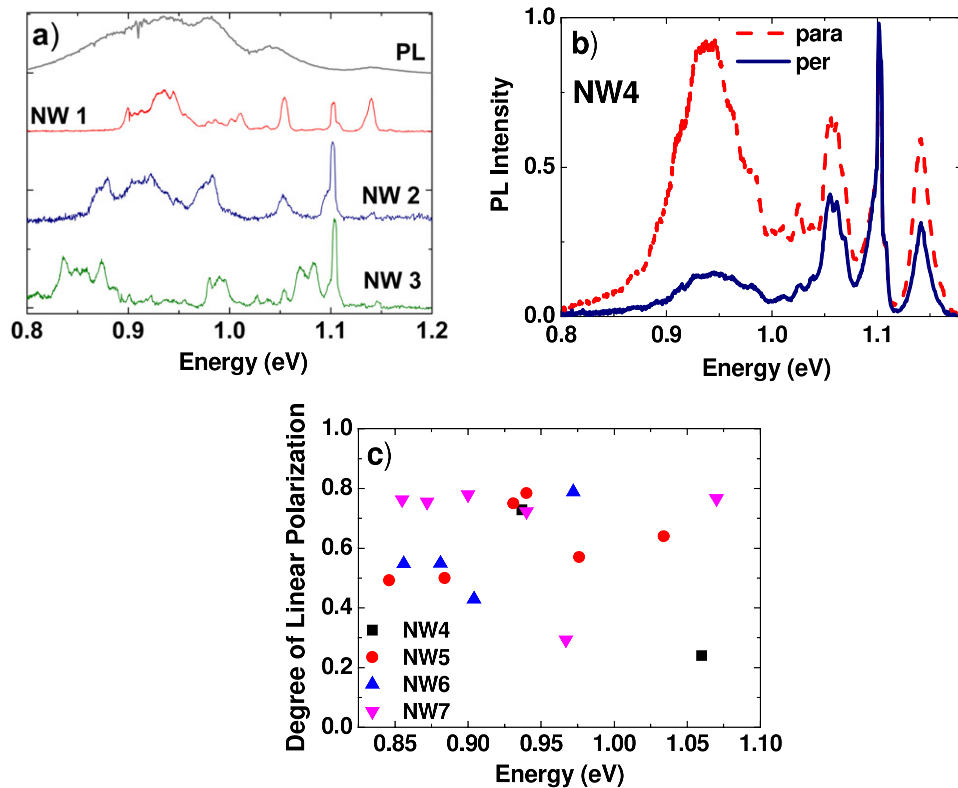

Figure 5. (a) Micro-PL spectra of several NWs (P_{ex} = 150 μW) compared with the PL of the NWs on the original substrate. (b) Emission of a NW as a function of the linear polarization: red dashed (blue solid) line polarization parallel (perpendicular) to the NW axis. (c) Degree of linear polarization studied as a function of the emission energy.

through the upper QW states, before it escapes to the barrier material [33].

In addition, we can observe that the room temperature PL peak's wavelengths for sample A and sample C are around 1.3 μm (0.954 eV) and 1.55 μm (0.8 eV), respectively (see the inset of figure 4). Other monolithic growth methods have been proposed for obtaining III–V semiconductors on silicon substrates using an $SrTiO_3$ (STO) template [34]. Our 20-fold reduction of the PL intensity is four times better than that obtained for InAsP/InP QW monolithically grown on STO/Si substrates [35]. This demonstrates the potential of the InP/InAs/InP core–shell NWs on Si substrates for the fabrication of emitters in the telecommunication wavelength range (1.3–1.55 μm) operating at room temperature.

5. Optical properties of single NWs

To improve our understanding of the NW optical properties, microphotoluminescence (micro-PL) experiments are performed on single InP/InAs/InP core–shell NWs. The NWs from sample B′ grown on Si(111) were transferred from their original substrate onto a new silicon substrate. The low NW density on the new substrate allows us to focus a laser beam on a single NW. Figure 5(a) shows the PL spectrum of the NWs on the original substrate and the micro-PL spectra of different single NWs for an excitation power of 150 μW. The peak observed around 1.1 eV on the micro-PL spectra is attributed to the silicon substrate. We assume that this peak is not observed in the PL spectra due to the high density of NWs. The micro-PL spectra of the single NWs are complex: several peaks or groups of peaks are observed for each individual NW. For instance, groups of peaks located around 0.88, 0.92, 0.98 and 1.05 eV are observed for NW2. The energies of these peaks are quite close to energy position of the PL peaks and shoulders associated with the ML fluctuations. Each group of peaks can thus be associated with a specific thickness of the QW. This result confirms the TEM studies: the QW does not have the same thickness on all the facets of a given NW.

The NW emission is also studied as a function of the linear polarization. If the situation is clear for pure ZB NWs (the light is polarized along the NW axis, such as for InP NWs [36, 37]), the situation seems more complicated for Wz NWs where different results have been obtained [38]. In the Wz phase, the p-like valence band is split into three different bands labelled A, B and C. The lowest energy recombination is associated with the recombination of an electron with a hole in the A band (the A-exciton). This transition is expected to be strongly polarized perpendicularly to the *c*-axis and, thus, to the NW axis. This result was observed for Wz InP NWs [36] but opposite results have also been observed for some Wz NWs [38, 39]. To our knowledge, the polarization dependence of the Wz InP/InAs/InP core–shell NW emission has never been obtained.

Figure 5(b) shows the PL emission of an individual NW for two polarization configurations: parallel (*c*-axis) and perpendicular (*a*-axis) to the NW axis. The maximum PL intensity is obtained for the linear polarization parallel to the

NW axis. The degree of linear polarization (DLP) is defined by the equation DLP $= (I_c - I_a)/(I_c + I_a)$, where I_c (I_a) is the intensity parallel (perpendicular) to the NW axis (the *c*-axis of Wz). The DLPs are equal to 73% (for the peak at 0.94 eV), 24% (1.06 eV) and 30% (1.14 eV). This result is similar to the DLP obtained for ZB InAs(P)/InP quantum wires and dashes where emission polarized along the wire/dash axis was reported with DLP in the 20–50% range [40, 41] but is in contradiction with the selection rule for the A-exciton for the Wz phase. Such polarization dependence has already been observed for Wz CdSe NWs without any core–shell structure [39]. We have to assume, as in [38], that the shape of the NW and, in our specific case, the shape of the InAs/InP QWs, has more impact on the polarization dependence than the selection rules of bulk Wz. Polarization-resolved measurements performed on several NWs reveal that the NW emission is mainly parallel to the NW axis and that the DLP seems independent of the emission energy (figure 5(c)). This result confirms the hypothesis of a DLP driven by the NW geometry. If the geometry is the key parameter, the DLP will depend on the ratio 'NW diameter/emission wavelength' [42]. Due to the small NW diameter (≈75 nm), the ratio is very small for all of the QW emission range (from 1100 to 1500 nm).

6. Conclusion

In summary, purely wurtzite InP/InAs/InP core–shell nanowires emitting in the telecommunication wavelength band were grown on (001)- and (111)-oriented silicon substrates using SSMBE. A long lifetime, in the 5–7 ns range, is measured at 14 K. Micro-PL measurements reveal the presence of localized states in the radial InAs quantum well and that the emission is mainly polarized along the nanowire axis. At room temperature, the PL intensity is equal to 5% of the 14 K PL intensity, confirming the good quality of the III–V material grown on silicon and the possibility of integrating efficient III–V semiconductor emitters such as laser diodes or single-photon emitters on silicon substrates.

Acknowledgment

We would like to thank M Hocevar from Delft University of Technology for helpful discussions on the transfer of nanowires.

References

[1] Duan X, Huang Y, Cui Y, Wang J and Lieber C M 2001 *Nature* **409** 66
[2] Huang Y and Lieber C M 2004 *Pure Appl. Chem.* **76** 2051
[3] Wagner R S and Ellis W C 1964 *Appl. Phys. Lett.* **4** 89
[4] Woo R L, Xiao R, Kobayashi Y, Gao L, Goel N, Hudait M K, Mallouk T E and Hicks R F 2008 *Nano Lett.* **8** 4664
[5] Mi Z, Yang J, Bhattacharya P, Chan P K L and Pipe K P 2006 *J. Vac. Sci. Technol.* B **24** 1519
[6] Balakrishnan G, Jallipalli A, Rotella P, Huang S, Khoshakhlagh A, Amtout A, Krishna S, Dawson L R and Huffaker D L 2006 *IEEE J. Sel. Top. Quantum Electron.* **12** 1636
[7] Dick K A *et al* 2006 *Nanotechnology* **17** 1344
[8] Paiman S *et al* 2009 *Nanotechnology* **20** 225606
[9] Tchernycheva M, Travers L, Patriarche G, Glas F, Harmand J C, Cirlin G E and Dubrovskii V G 2007 *J. Appl. Phys.* **102** 094313
[10] Cornet D M, Mazzetti V G M and LaPierre R R 2007 *Appl. Phys. Lett.* **90** 013116
[11] Gudiksen M S, Lauhon L J, Wang J, Smith D C and Lieber C M 2002 *Nature* **415** 617
[12] Panev N, Persson A I, Skold N and Samuelson L 2003 *Appl. Phys. Lett.* **83** 2238
[13] Mohan P, Motohisa J and Fukui T 2006 *Appl. Phys. Lett.* **88** 133105
[14] Masumoto Y, Goto K, Yoshida S, Sakuma Y, Mohan P, Motohisa J and Fukui T 2010 *Phys. Rev.* B **82** 075313
[15] Sköld N, Pistol M E, Dick K A, Pryor C, Wagner J B, Karlsson L S and Samuelson L 2009 *Phys. Rev.* B **80** 041312
[16] Tchernycheva M, Cirlin G E, Patriarche G, Travers L, Zwiller V, Perinetti U and Harmand J C 2007 *Nano Lett.* **7** 1500
[17] Moewe M, Chuang L C, Crankshaw S, Ng K W and Hasnain C C 2009 *Opt. Express* **17** 7831
[18] Mattila M, Hakkarainen T, Mulot M and Lipsanen H 2006 *Nanotechnology* **17** 1580
[19] Minot E D, Kelkensberg F, Kouwen M, Dam J A, Kouwenhoven L P, Zwiller V, Borgström M T, Wunnicke O, Verheijen M A and Bakkers E P A M 2007 *Nano Lett.* **7** 367
[20] Leonelli R, Tran C A, Brebner J L, Graham J T, Tabti R, Masut R A and Charbonneau S 1993 *Phys. Rev.* B **48** 11135
[21] Folliot H, Loualiche S, Lambert B, Drouot V and Le Corre A 1998 *Phys. Rev.* B **58** 10700
[22] Zanolli Z, Fuchs F, Furthmüller J, von Barth U and Bechstedt F 2007 *Phys. Rev.* B **75** 245121
[23] Bao J, Bell D C, Capasso F, Erdman N, Wei D, Froberg L, Martensson T and Samuelson L 2009 *Adv. Mater.* **21** 3654
[24] De A and Pryor C E 2010 *Phys. Rev.* B **81** 155210
[25] Tomimoto S, Kurokawa A, Sakuma Y, Usuki T and Masumoto Y 2007 *Phys. Rev.* B **76** 205317
[26] Pal B, Goto K, Ikezawa M, Masumoto Y, Mohan P, Motohisa J and Fukui T 2009 *Appl. Phys. Lett.* **95** 232116
[27] Friedler I, Sauvan C, Hugonin J P, Lalanne P, Claudon J and Gérard J M 2009 *Opt. Express* **17** 2095
[28] Bleuse J, Claudon J, Creasey M, Malik N S, Gérard J-M, Maksymov I, Hugonin J-P and Lalanne P 2011 *Phys. Rev. Lett.* **106** 103601
[29] Wei Q Y, Li T, Wu Z H and Ponce F A 2010 *Phys. Status Solidi* a **207** 2226
[30] Popescu D P, Eliseev P G, Stintz A and Malloy K J 2004 *Semicond. Sci. Technol.* **19** 33
[31] Lei H P, Wu H Z, Lao Y F, Qi M, Li A Z and Shen W Z 2003 *J. Cryst. Growth* **256** 96
[32] Cheng J *et al* 2009 *Appl. Phys. Lett.* **95** 232116
[33] Ilahi B, Sfaxi L and Maaref H 2007 *J. Lumin.* **27** 741
[34] Saint-Girons G, Cheng J, Regreny P, Largeau L, Patriarche G and Hollinger G 2009 *Phys. Rev.* B **80** 155308
[35] Gobaut B, Penuelas J, Cheng J, Chettaoui A, Largeau L, Hollinger G and Saint-Girons G 2010 *Appl. Phys. Lett.* **97** 201908
[36] Mishra A *et al* 2007 *Appl. Phys. Lett.* **91** 263104
[37] Wang J, Gudiksen M S, Duan X, Cui Y and Lieber C M 2001 *Science* **293** 1455
[38] Lew Yan Voon L C, Zhang Y, Lassen B, Willatzen M, Xiong Q and Eklund P C 2008 *J. Nanosci. Nanotechnol.* **8** 1
[39] Shan C X, Liu Z and Hark S K 2006 *Phys. Rev.* B **74** 153402
[40] Yang H, Mu X, Zotova I B, Ding Y J and Salamo G 2002 *J. Appl. Phys.* **91** 3925
[41] Salem B, Olivares J, Guillot G, Bremond G, Brault J, Monat C, Gendry M, Hollinger G, Hassen F and Maaref H 2001 *Appl. Phys. Lett.* **79** 4435
[42] Ruda H E and Shik A 2006 *J. Appl. Phys.* **100** 024314